Multiwavelength Analysis of the Kinetics of Reduction of Cytochrome aa_3 by Cytochrome *c*

Richard W. Hendler, Salil K. Bose, and Richard I. Shrager*
Laboratory of Cell Biology, National Heart, Lung, and Blood Institute; *Division of Computer Research and Technology, National Institutes of Health, Bethesda, Maryland 20892 USA

ABSTRACT Some new approaches to the kinetic study of the reduction of cytochrome aa_3 by cytochrome *c* are presented. The primary innovations are the use of a spectrometer which can acquire multiwavelength data as fast as every 10 μs, and the application of a variety of analytical methods which can utilize simultaneously all of the time-resolved spectral data. These techniques include singular value decomposition (SVD), deconvolutions based on pure Gaussian models for absorption peaks, deconvolutions based on isolated absorption spectra for the pure components, and simulations of SVD-deduced and actual experimental difference spectra. The reduction characteristics of the anaerobic resting enzyme can be distinguished from those of pulsed forms. In the former case, only two electrons can be bound by cytochrome aa_3, whereas in the latter case complete reduction of the enzyme is achieved.

INTRODUCTION

Cytochrome aa_3 is the terminal member of the respiratory chain. It accepts four electrons from cytochrome *c* and reduces a molecule of O_2 to form H_2O. The energy released in this electron transfer is used to pump protons across a membrane, forming an electrochemical potential for protons, which drives the synthesis of ATP (see Wikström et al., 1981). During the process of loading of oxidized cytochrome aa_3 with electrons from cytochrome *c*, all of the spectra from the oxidized and reduced forms of all of the intermediates overlap and grow and diminish with rate constants, which themselves may not be the same under all conditions. To understand the individual kinetic steps in the process, a powerful means of deconvolution must be employed. Facing a similar situation during studies of the potentiometric behavior of cytochrome aa_3, we have found that the availability of complete optical spectra, rather than only single or double absorbances at discrete wavelengths, and the application of analytical techniques, capable of using all of the spectral data, were invaluable in the deconvolution of overlapping spectra into the individual components (Shrager and Hendler, 1982; Hendler et al., 1986). The purpose of the present investigation was to re-examine the kinetics of cytochrome aa_3 reduction by cytochrome *c*, using a new kind of spectrometer which can acquire continuous spectra rapidly in time from a single sample, and a group of analytical techniques capable of utilizing all of the spectral information. With these new approaches we have been able to confirm earlier findings on the kinetics of transfer of the first electron from cytochrome *c* to cytochrome *a*, and to extend the kinetic treatment to follow the binding of all four electrons to the pulsed form of cytochrome aa_3.

Received for publication 2 March 1993 and in final form 11 June 1993.

0006-3495/93/09/1307/11 $2.00

EXPERIMENTS AND COMPUTATIONS

General

Cytochrome aa_3 was isolated from beef heart by the method of Yoshikawa et al. (1977) as described in Pardhasaradhi et al. (1991). The turnover number was determined in two ways. The rate of cytochrome *c* oxidation as a function of cytochrome *c* concentration (from 5 to 40 μM) was measured spectrophotometrically at 550 nm, in a solution containing 5 nM cytochrome aa_3 and 50 mM potassium phosphate at pH 7.4 and 22°C. The measured K_m was 5–10 μM. Alternatively, the initial rate of O_2 uptake was measured polarographically with a Clark-type electrode (YSI-5331; YSI, Inc., Yellow Springs, OH) in a solution containing cytochrome *c* (5–40 μM), ascorbate (1 mM), N,N,N′,N′-tetramethyl-*p*-phenylenediaminedihydrochloride (TMPD) (100 μM), and 62.5 μM cytochrome aa_3 in 50 mM potassium phosphate at pH 7.4 and 22°C. The turnover number was 40–50 s^{-1} in both assays and is comparable to published values under the same conditions (Wilms et al., 1980).

Description of the spectrometer and stopped-flow apparatus

The spectrometer was developed and built at the National Institutes of Health (NIH) in collaboration with Walter S. Friauf, John Cole, and Paul D. Smith of the Biomedical Engineering and Instrumentation Program, National Center for Research Services (NCRR), NIH, and Hal A. Fredrickson of the Computer Systems Laboratory, Division of Computer Research and Technology (DCRT), NIH. The instrument will be described in detail in a separate publication. Only essential details about its capabilities and operation will be described here. Two separate 1/4-m spectrographs with ruled gratings (Oriel Corp., Stratford, CT, Models 77200 and 77233 (1200 lines/mm)) were used. The spectrographs were modified to accept two 46-photodiode arrays (s4112-46Q; Hamamatsu, Bridgewater, NJ) as detectors. Each spectrograph was capable of covering a spectral range of 130 nm with a resolution of 2.9 nm. To achieve the most rapid throughput of data, each photodiode (or channel) was provided with its own 12-bit A/D converter (AD1678; Analog Devices, Norwood, MA) and 1024-deep FIFO buffer (IDT 7202; Integrated Device Technology, Santa Clara, CA). The time for data acquisition was set at 8.6 μs, and the readout of accumulated charges at 1.4 μs, allowing for a maximum time resolution of 10 μs. The operation of the spectrometer was under computer control. Although all of the spectra taken in the present work used the 10-μs interval, the data collection period could be increased as needed. In a single experiment, up to 1024 spectra can be acquired either continuously or with timed intervals between spectra

varied from 10 μs to 21 s. Each channel was individually calibrated with known transmittance neutral density filters to allow conversion of transmittance to absorbance. Electronic circuitry controlled and coordinated the operation of the stopped flow apparatus and the start of data acquisition and conversion.

The stopped-flow apparatus ("Aminco-Morrow") was purchased from the American Instrument Co., Silver Spring, MD (now SLM-Aminco, Urbana, IL). Each of the two cylinders of this instrument is connected to a Hamilton gas-tight two-way valve. This allows the cylinder to be communicative with either an external syringe connected to the valve or with the reaction chamber where the kinetics are observed. To help ensure anaerobiosis we made the following modifications. The two-way Hamilton valves were replaced by three-way valves which allowed communication between the cylinders of the stopped flow device and specially constructed anaerobic bottles. The bottles (~17 × 80 mm) had 10-ml capacities and were built in the glass and instrument shops at NIH. They were individually connected to the stopped-flow cylinders by stainless steel tubing and Swage-Lok fittings. Each bottle contained a magnetic "flea" and sat above a magnetic stirring motor. A sidearm at the bottom of each bottle contained an O_2 electrode (Model MI-730; Microelectrodes, Inc., Londonderry, NH). The electrodes were individually connected to an O_2 meter (Model OM-4; Microelectrodes, Inc., Londonderry, NH). The outputs of the meters were sent to two channels of a chart recorder for continuous monitoring of O_2 levels in the bottles. The bottles were provided with two separate means for passing N_2 gas into and above the solution. A long hypodermic needle was inserted into a gas-tight port at the top of the bottle. This needle could be raised and lowered into and out of the solution. Gas could be either bubbled through the buffer or played on top of the solution. The needle was also used to introduce components into the solution. A separate flow of gas was continuously maintained through the bottle from an additional side arm.

Experimental protocol

10 ml of 50 mM potassium phosphate, pH 7.4, was taken into each of two glass syringes and the syringes were inserted, without their plungers, into the external Luer-lok outlets of the three-way gas-tight Hamilton valves attached to the cylinders and anaerobic bottles of the stopped-flow apparatus. Nitrogen gas (99.995% minimum purity) was passed through both the hypodermic needles and sidearm inlets of the empty anaerobic bottles and then through the Hamilton valves to the buffers in the open glass syringes for 15 min. In this way, the bottles, connecting lines, and buffers could be purged simultaneously. The plungers were then fixed to the syringes and the buffers forced through the gas-tight valves, directly into the reservoir bottles. The valves were then closed and N_2 was passed both over and directly through the solutions in the bottles, until the O_2 electrodes recorded zero signal. The solutions were then transferred directly to the cylinders of the stopped-flow device and immediately back to the anaerobic bottles. A small O_2 reading was noted in the solution, which decreased to zero as the gas flow continued. The process was repeated a few times until no O_2 reading was observable. Anaerobic buffer (~3 ml) was then passed to the cylinder, and afterwards expelled through the reaction chamber. This process was repeated a second time, leaving ~4 ml of buffer in the bottles. The hypodermic needle was raised to just above the buffer solution and stock solutions of the reactants were introduced to each side as N_2 was continuously flowed through the side arms. One side received 42 μl of 1.0 M cytochrome aa_3, and the other 105 μl of 1 mM cytochrome *c* and 45 μl of 0.5 M ascorbate. The solutions were held until the O_2 electrodes showed zero readings, and then each cylinder was loaded with the anaerobic reactants. The reactant solutions were mixed in a 1:1 ratio producing final concentrations of close to 2.3 μM cytochrome aa_3, 12.5 μM cytochrome *c*, and 5.0 mM ascorbate.

Oxygen integrity of the system

When an O_2-free solution was taken into either of the working cylinders of the stopped-flow device, and immediately dispelled back into the anaerobic reservoir, ~0.4 μM O_2 was observed in the solution. What proportion of this [O_2] was acquired from the cylinder or while in transit between the cylinder and reservoir cannot be said. Upon remaining in the cylinder, the solution acquired O_2 at a rate of ~7 nM/min. When it was desired to introduce low levels of O_2 into the system, the solution was taken directly from the cylinder into a plastic syringe attached to the cylinder block through a Hamilton gas-tight valve and held for a period of time before being returned to the cylinder. The O_2 concentration of the solution increased at a rate of 0.2–0.3 μM min^{-1} as a result of the transfer of O_2 through the plastic wall of the syringe. The immediate transfer of solution from the cylinder to the plastic syringe and back introduced a level of 0.2–0.3 μM O_2 to the solution.

Computations

Singular value decomposition uses all of the spectral and kinetic information to define transitions occurring in time, in terms of difference spectra and kinetic constants. It does not identify, however, the individual molecular species undergoing the transitions. A major challenge is to deconvolute the experimentally obtained combined spectra into individual spectra for the reduced and oxidized species of cytochromes *a*, a_3, and *c*. The problem is that individual model spectra for isolated cytochromes *a* and a_3 are not available. Two separate computational approaches were used to deconvolute the kinetic data into changes for the individual cytochromes. Both are based on the use of the pseudoinverse operator of linear algebra, and are described in a separate paper (Hendler and Shrager, 1993). In principle, if fundamental component spectra are known and included as columns in a matrix, *D*, the titration profiles can be computed in a matrix, *F*, whose transpose is obtained by multiplying a matrix of raw experimental spectra *AB* by the pseudoinverse of matrix *D*. In the present work, both Gaussian shapes and deduced whole spectra for cytochromes *a* and a_3 were used. Additional details will be provided upon request.

Other

All computations and curve fitting were performed on a PC using either 386-MATLAB (The MathWorks, Inc., Natick, MA) or MLAB (Civilized Software, Inc., Bethesda, MD). All of the figures were produced using MLAB.

RESULTS

Analysis of trends of reduction for heme *a* and a_3 centers using deconvolutions based on Gaussians

The reduction of cytochrome aa_3 by cytochrome *c*, under anaerobic conditions was followed for 25 min, using 10-μs data collection windows for acquiring spectra separated by a series of increasing time intervals. The entire series was comprised of 864 spectra. For the first 33 s, 754 sequential spectra were collected. During the later times, where very little change was occurring, groups of 10 spectra each were collected, spaced by relatively large time intervals.

The Gaussian analysis technique was used to help determine the extent and nature of the changes occurring throughout the entire time course. Fig. 1 *D* shows that in the first time sample, the enzyme was nearly 25% reduced and this was completely accounted for by cytochrome *a*. It is also seen that in the dead time of the instrument (~3 ms), ~2.2 μM cytochrome *c* was oxidized. Therefore, in the first kinetic phase, which was mostly completed in the dead time of the stopped-flow apparatus, one electron equivalent was transferred from cytochrome *c* to cytochrome *a*. However only one half of the cytochrome *a* was reduced (i.e., the percent of total reduction

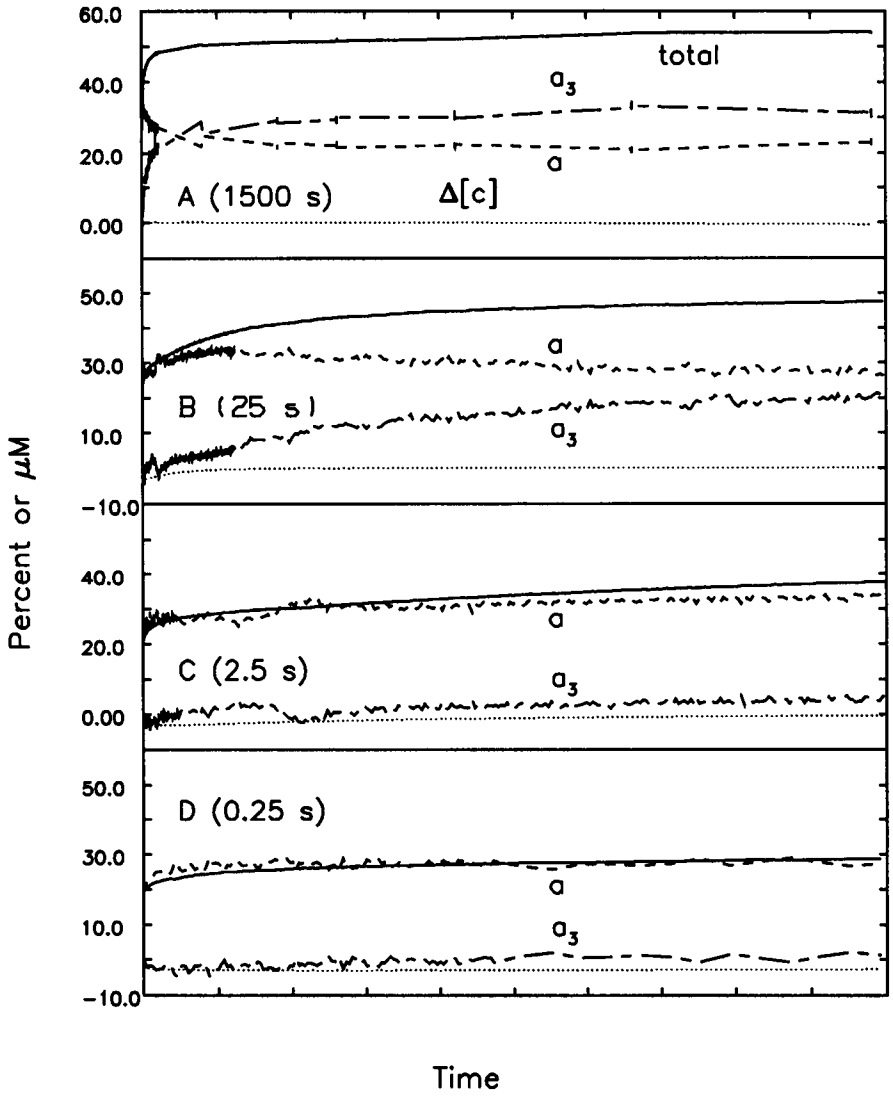

FIGURE 1 Time course of reduction of cytochromes *a* and a_3 in the resting enzyme by cytochrome *c*, analyzed by Gaussian deconvolution: The reduction of resting cytochrome aa_3 by cytochrome *c* was followed over a 25-min period. One cylinder of the stopped-flow apparatus contained oxidized cytochrome oxidase and the other ascorbic acid and reduced cytochrome *c*. After mixing, the concentrations were 2.1 μM, 12.5 μM, and 5 mM, respectively, for cytochrome aa_3, cytochrome *c*, and ascorbate. The buffer was 50 mM potassium phosphate at pH, 7.4. Spectra were collected in 10-μs windows with spacings staggered from 1 ms in the early part to 100 ms, at 10 ms to 3 s, at 100 ms to 393 s, and at 1 s to the end. The record is presented in four different time scales: 0–250 ms in *D*, 0–2.5 s in *C*, 0–25 s in *B*, and 0–1500 s in *A*. The percent of reduced cytochrome aa_3 accounted for by *a*, pct*a* (*short dashed line*), and by a_3, pcta_3 (*alternating short* and *long dashed line*), and total percent (*a* plus a_3) are shown, as well as the incremental change in concentration of reduced cytochrome *c* compared to the starting concentration of 12.5 μM (*dotted line*). The *y*-axis scale for change in cytochrome *c* concentration is micromolar.

of cytochrome aa_3 accounted for by cytochrome *a* (pct*a*) = 25% instead of 50%). This most likely means that the one electron was time-shared between heme *a* and Cu_A. The electron transfer from cytochrome *c* to cytochrome *a* continued at a slower pace with a maximum level of cytochrome *a* reduction (i.e., pct*a* = ~33%) reached at ~2.5 s (Figs. 1, *C* and *B*). Thereafter, pct*a* declined to 22% as pcta_3 (i.e., the percent of total reduction of cytochrome aa_3 accounted for by cytochrome a_3) rose from 8 to 29%, indicating electron transfer from *a* to a_3 (Fig 1 *A*). During the long incubation (i.e., 25 min), plateaus of ~50% for the total level of reduction of cytochrome aa_3 and ~25% each for pct*a* and pcta_3 were approached (Fig. 1 *A*).

When the enzyme is 100% reduced, each heme *a* and heme a_3 account for 50% of the total heme absorbance (i.e., pct*a* = pcta_3 = 50%). Therefore, the 25% levels shown in Fig. 1 each account for one half electron equivalent. The level of cytochrome aa_3 reduction increased from 25% at zero observation time (one electron bound) to ~50% at the end of 25 min. If two electrons were bound and a total of only one electron is accounted for by the levels of heme reduction, it appears that for the resting enzyme, under anaerobic conditions, electron transfer from cytochrome *c* to cytochrome aa_3 is severely inhibited when each of the two heme-Cu pairs contain and share one electron. It is important to note that this was true even though fully reduced (12.5 μM) cytochrome *c* was present.

At the end of the time course shown in Fig. 1 (i.e., at 1500 s), a small amount of O_2 was allowed to enter the system by opening and closing the external valve that connects to the take-up syringe. The effects of this action are shown in Fig. 2, where the entire incubation is presented. The first spectrum taken after opening the valve (at 1500 s) shows an abrupt increase in the level of reduction of cytochrome *a* accompanied by a concomitant oxidation of cytochrome *c* and no increase in the level of reduction of cytochrome a_3. Afterwards, pct*a* declined as pcta_3 rose. The level of reduction of cytochrome aa_3 was ~90% and still rising at the end of the observation period, while an apparent transfer of electrons from cytochrome *a* to cytochrome a_3 was in progress.

In order to obtain more information on the precise effects of O_2 on the kinetics of the reduction processes, a series of

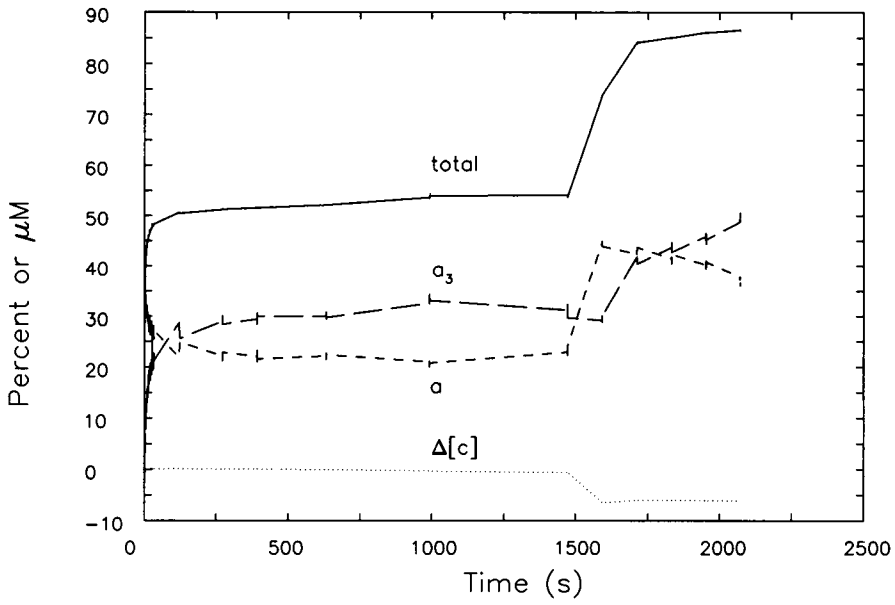

FIGURE 2 Conversion of "resting" to "pulsed" enzyme: The experiment shown in Fig. 1 is presented here with the additional record obtained after opening the valve to the takeup syringe and expelling port, at 1500 s. Refer to the legend to Fig. 1 for additional details.

experiments were performed with gradually increasing amounts of O_2 present. Fig. 3, *A–F*, depicts a series of six experiments performed in the presence of increasing amounts of O_2. It is immediately evident that O_2 elicits and augments the appearance of phases in which electrons appear to move first from cytochrome *a* (*dashed line*) to a_3 (*dotted line*), (from ~0.02 to 1 s), and then back from cytochrome a_3 to *a* (from ~1 to 10 s). At the highest levels of O_2 (*E* and *F*), a steady state is reached in which, cytochrome *a* appears to be completely oxidized, while cytochrome a_3 appears to be substantially reduced. At the termination of the steady state, the enzyme proceeds to full reduction. The figure also shows that coincident with the start of apparent transfer of electrons from cytochrome *a* to a_3, there is an increased oxidation of cytochrome *c* (*short* and *long dashed line*) and, the higher the amount of O_2 present, the greater the extent of oxidation of cytochrome *c*. The presence of the generally higher amounts of O_2 disturbed the Gaussian fittings at the start, such that initial pcta_3 values were slightly negative and initial pct*a* values were higher than the 25% seen at lower $[O_2]$.

The major trends in electron binding by the enzyme seen in these experiments, based on the Gaussian deconvolutions and resulting identifications of reduced cytochromes *a* and a_3, are electron transfer; 1) from cytochrome *c* to cytochrome *a* (*c*→*a*), 2) from cytochrome *a* to cytochrome a_3 (*a*→a_3), and 3) from cytochrome a_3 back to cytochrome *a* (a_3→*a*), before 4), the final complete reduction of the enzyme. Phases 1, 2, and 4, are entirely consistent with what is already known about the reduction process. The indicated transfer of electrons from cytochrome a_3 back to cytochrome *a* is unexpected and requires more study.

Analysis of trends of reduction for heme *a* and a_3 centers using deconvolutions based on spectra

The same experiments shown in Fig. 3 were next analyzed by the pseudoinverse deconvolution method based on the deduced difference spectra for the individual redox centers (Fig. 4). Although not identical, this analysis does confirm many of the observations obtained in the Gaussian analysis as follows: 1) In all cases, the enzyme went to full reduction, 2) Increasing amounts of O_2 heightened the appearance of an apparent transfer of electrons from cytochrome *a* (*dashed line*) to cytochrome a_3 (*dotted line*) in the time range of ~0.05 to ~0.8 s, 3) Coincident with the increased electron transfer from *a* to a_3, there was an increase in the extent of oxidation of cytochrome *c* (*short* and *long dashed line*), 4) At the highest levels of O_2, a steady state was reached which abruptly ended, and then the enzyme proceeded to full reduction (*E* and *F*). The important differences are that in the steady state, cytochrome a_3 appears much more oxidized than found in Fig. 3, and that instead of a drop in the amount of reduced cytochrome a_3 as the level of reduced cytochrome *a* rose in the time range of 1 to 15 s, a lag in the rate of reduction was seen (Fig. 4 *C*). In these deconvolutions, the starting level of reduced cytochrome *a* is at the one half level as seen in the time courses with lower amounts of O_2 present, and the level of reduced cytochrome a_3 is not negative (cf. Fig. 3).

Comparison of simulated and actual difference spectra to help identify electron transfers events

The full application of SVD requires fitting of the vectors of the *V* matrix by a mathematical model (Hendler and Shrager, 1993). For cases where the O_2 level was extremely low, a multiexponential model provided excellent fits. At higher levels of O_2, the quality of the fits using a multiexponential deteriorated. In order to verify and further identify the individual electron transfer events discerned both by deconvolutions based on the pseudoinverse and by SVD the technique of simulation using isolated spectra was applied. For this purpose, an experiment was chosen in which the presence of O_2 was large enough to show the several phases of

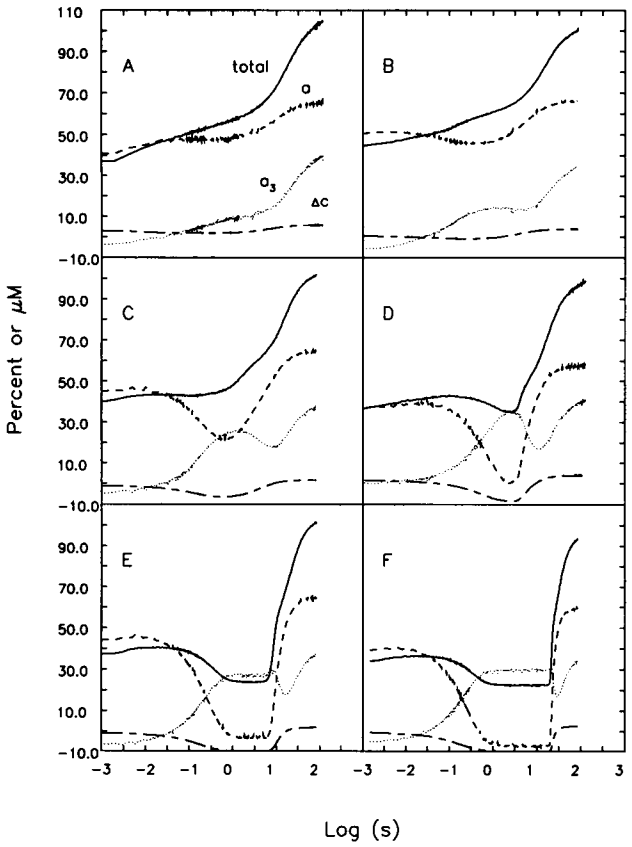

FIGURE 3 Effects of O_2 on the time course of cytochrome aa_3 reduction analyzed by the pseudoinverse deconvolution using Gaussians: *A–F* represent experiments performed in the presence of progressively higher concentrations of O_2. The level of O_2 was regulated as described in the text. Approximate levels of $[O_2]$ were <1.0, <1.0, 3, 4, 5, and 7 μM for *A–F*, respectively. The ordinate shows the percent of total reduction of the hemes in cytochrome aa_3, or the change in μM of reduced cytochrome *c*. The solid line is the sum of the two discontinuous lines labeled *a* (*dashed*) and a_3 (*dotted*) for cytochromes *a* and a_3, respectively. The alternating long and short dashed line (Δ*c*) in the lower part of the panels shows the change in concentration of reduced cytochrome *c* in μM referred to the units on the ordinate, where *0* represents 12.5 μM (the usual starting concentration). The actual reading, therefore, records μM changes from 12.5 μM.

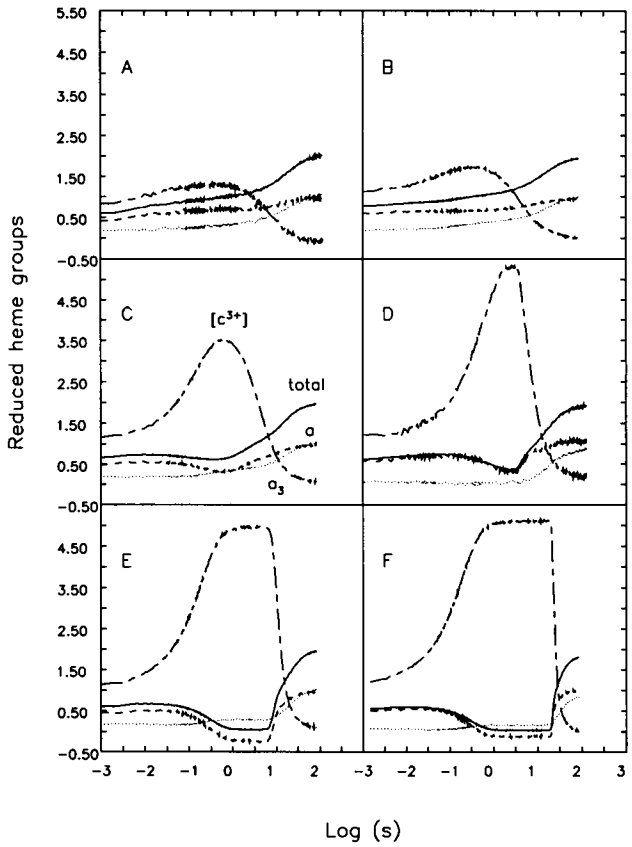

FIGURE 4 Effects of O_2 on the time course of cytochrome aa_3 reduction analyzed by the pseudoinverse deconvolution using spectra: The experiments shown in this figure are the same as those shown in Fig. 3. The ordinate is in units of reduced heme groups in cytochrome aa_3. The solid, dashed, and dotted lines represent total heme, heme *a*, and heme a_3, respectively, as in Fig. 3. The $[c^{3+}]$ line shows the amount of cytochrome *c* oxidized, in electron equivalents to heme groups. Thus, for these experiments with 2.5 μM cytochrome aa_3 present, the 12.5 μM cytochrome *c* equals 12.5/2.5 = 5 electron equivalents.

electron transfers by the Gaussian analysis (Fig. 5), but low enough to obtain satisfactory fits with the multiexponential model.

Fig. 6 *A* shows the difference spectrum, obtained from SVD, for the initial fast process, which was identified above as $c \rightarrow a$. A corresponding difference spectrum (5.5–0 ms) taken from the raw data is shown in Fig. 6 *B*. The negative peaks at 410, 520, and 550 nm represent the oxidation of cytochrome *c* and the positive peaks at 446 and 605 nm, the reduction of cytochrome *a*. Fig. 7 *A* shows an oxidized minus reduced difference spectrum for pure cytochrome *c*. A simulated difference spectrum for an electron transfer from cytochrome *c* to cytochrome *a* was constructed from the difference spectrum for cytochrome *c* shown in Fig. 7 *A*, and the difference spectrum for cytochrome *a* deduced by the Gaussian procedures. This simulated difference spectrum for $c \rightarrow a$ shown in Fig. 7 *B*, is quite similar to the two shown in Fig. 6, *A* and *B*. Fig. 6 *C* shows the difference spectrum deduced by SVD for the transfer identified by the pseudoinverse deconvolution techniques as $a \rightarrow a_3$. A difference spectrum (480–20 ms) obtained from the actual data is shown in Fig. 6 *D*. A negative peak is seen at 606 nm in both spectra. This is consistent with a transfer of electrons from cytochrome *a* to cytochrome a_3. If both cytochromes *a* and a_3 contributed equally to the Soret region, there should be no change at 446 nm. However comparing Fig. 6, *C* and *D*, to Fig. 7 *A* for pure cytochrome *c*, shows that some positive absorbance has been added to the 446-nm region. A simulated difference spectrum for the transfer of an electron from cytochrome *a* to cytochrome a_3 was produced from the individual deduced difference spectra by the Gaussian procedures. To account for the rise in absorbance at 446 nm seen in Fig. 6, *C* and *D*, the contributions of cytochromes a_3 and *a* to the 446-nm region were set at 60 and 40%, respectively. This difference spectrum was then added to the oxidized minus reduced cytochrome *c* spectrum shown in Fig. 7 *A*. The resulting simulated difference spectrum is shown in Fig. 7 *C*. It is remarkably similar to the experimental spectra shown in Fig. 6, *C* and *D*. Simulations were also made using the dif-

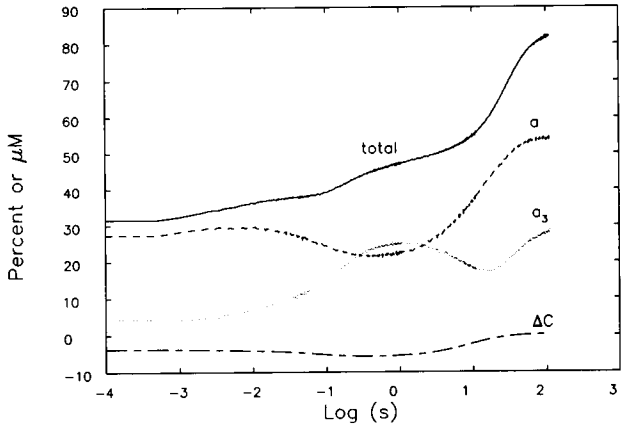

FIGURE 5 Time course of cytochrome aa_3 reduction in an experiment, at an intermediate level of $[O_2]$, analyzed by deconvolution using Gaussians: The short dashed line shows the percent of total heme reduction accounted for in cytochrome *a* (pct*a*). The dotted line represents cytochrome a_3 (pcta_3). The solid line is the sum of pct*a* and pcta_3. The bottom alternating short and long dashed line is the change from 12.5 μM in the concentration of cytochrome *c*.

ference spectra for cytochromes *a* and a_3 obtained from the procedures based on whole spectra (Computations Section). The difference spectrum obtained in this manner is shown in Fig. 7 *D*. It too, resembles the spectra shown in Fig. 6, *C* and *D*. The difference spectrum obtained by SVD for the apparent $a_3 \rightarrow a$ electron transfer is shown in Fig. 6 *E*, and Fig. 6 *F* shows the corresponding difference spectrum, 15–2 s, obtained from the raw data. In Fig. 6 *E*, the increase in absorbance at 605 nm occurred with a decrease at 446 nm. This is consistent with the observations on the $a \rightarrow a_3$ electron transfer, where it was concluded that the Soret absorbance is somewhat stronger in cytochrome a_3 than in cytochrome *a*. The difference spectrum shows the increase at 605 nm, but the trough at 446 nm is not evident. The difference spectrum using raw data is contaminated by other changes overlapping the same time span, whereas the SVD spectrum represents a unique process. At any rate, the absence of a prominent peak at 446 nm in the difference spectrum shows that the process is not just the simple binding of electrons to either or both of cytochromes *a* and a_3. In this time span, cytochrome *c* is simultaneously undergoing reduction by ascorbate (tau = ~6 s). The simulated difference spectrum for $a_3 \rightarrow a$, based on Gaussians is shown in Fig. 7 *E*, and the one based on whole spectra is shown in Fig. 7 *F*. Both of these simulated spectra are very similar to the SVD obtained spectrum in Fig. 6 *E*, attributed to the $a_3 \rightarrow a$ electron transfer.

The comparisons of all of the difference spectra obtained by SVD, the use of experimental data, and two different kinds of simulation, support the conclusion reached using the Gaussian analysis procedure that a transfer of electrons from cytochrome a_3 to cytochrome *a* may have occurred. However, as we discuss below ("Discussion") there is an alternative explanation for this observation.

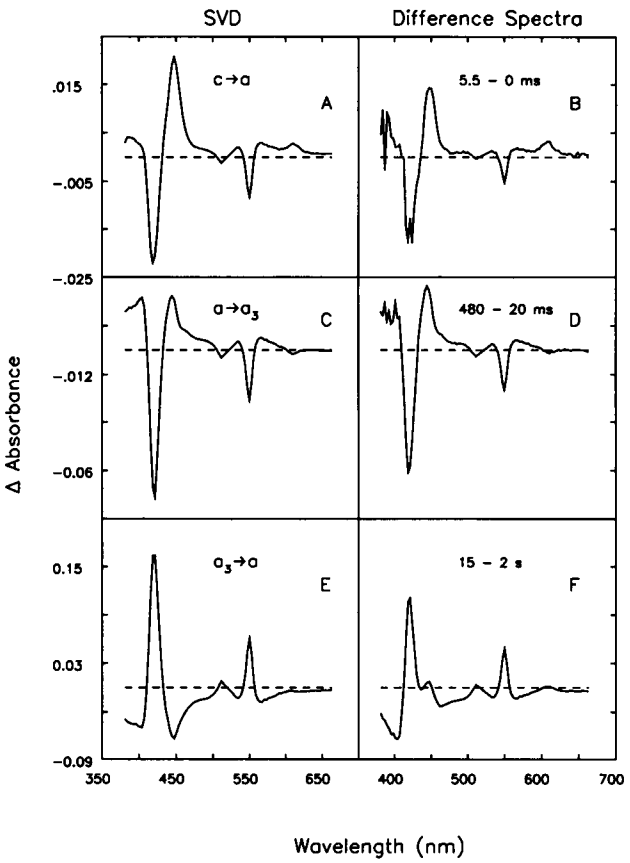

FIGURE 6 Spectral changes for major electron transfer events in the reduction of cytochrome aa_3 by cytochrome *c*: Difference spectra for specific kinetic phases were obtained by SVD analysis (*left-hand panels*) and compared with actual difference spectra obtained from the raw data, over time spans appropriate to the time constants for the particular kinetic phases obtained by the SVD analysis (*right-hand panels*). The data used were from the experiment shown in Fig. 5.

Determination of kinetic constants for electron transfers using SVD

The SVD analysis produces a matrix of time course eigenvectors for each of the principal basis spectra. These kinetic vectors are then simultaneously fit to a sum of exponentials plus a baseline. A summary of the phases seen for the resting enzyme under the most anaerobic conditions is presented in Table 1. The first phase is so rapid that most of it occurs in the dead time (~3 ms) of the stopped-flow apparatus. The pseudo first order kinetic constant, ~200 s^{-1}, corresponds to a time constant between 3.1 and 8.4 ms. The second order kinetic constant is $\sim 2 \times 10^7\ M^{-1}\ s^{-1}$. The SVD and Gaussian analyses identify this step as an electron transfer from cytochrome *c* to cytochrome *a*. Although SVD discerned (at least) five kinetic phases with the resting enzyme, most of the electron transfer occurred in the first and fifth phases. In the fifth phase, the Gaussian analysis identified an electron transfer from cytochrome *a* to a_3. Fig. 1 shows that in addition to the specific electron transfers seen in the first and fifth phases, there was a continuing slow net addition of electrons from cytochrome *c* to cytochrome aa_3, which increased the level of reduction from ~25% at the start to ~50% at the end.

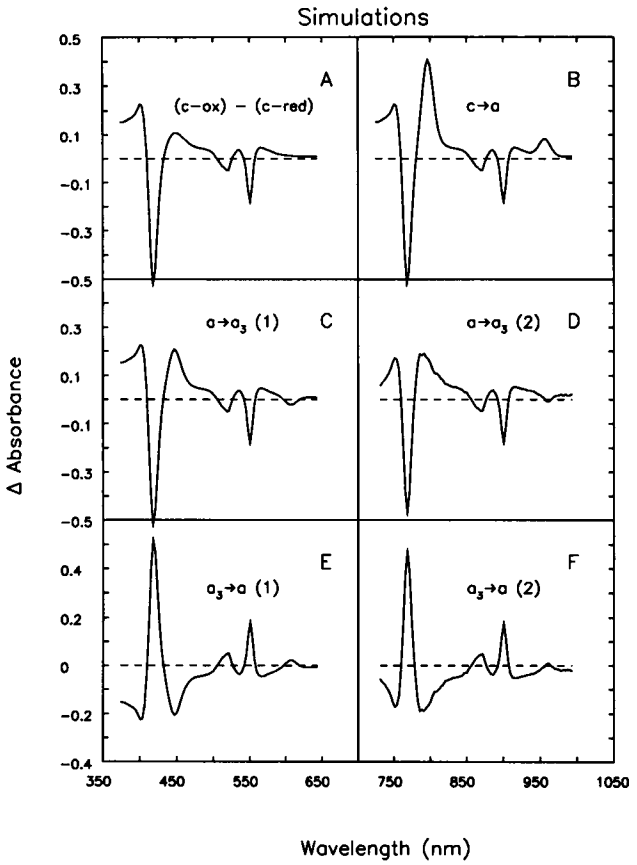

FIGURE 7 Simulations of spectral changes for the major electron transfer events in the reduction of cytochrome aa_3 by cytochrome *c*: *A* shows an oxidized minus reduced difference spectrum obtained with 12.5 μM cytochrome *c*. *B*, *C*, and *E*, were constructed by combining the difference spectrum of *A* with simulated difference spectra for cytochrome *a* (sima) and for cytochrome a_3 (sima3). The simulated spectra for cytochromes *a* and a_3 were made by using pure Gaussian shapes with midpoints at 446.5 and 606.4 and the corresponding half-height widths. For sima, the ratio of amplitudes at 605 and 446 nm was set at 0.24 and for sima3, it was 0.0484. Simulated difference spectra for $a \rightarrow a_3$ and $a_3 \rightarrow a$ electron transfers were made using sima3 and sima in a ratio of 1.5 to 1.0 (i.e., 60% Soret absorbance for a_3 and 40% for *a*). The simulated difference spectrum for $c \rightarrow a$ (*B*) was made by adding sima to the spectrum of panel A. The simulated spectrum for $a \rightarrow a_3$ (*C*) was made by adding the simulated difference spectrum for electron transfer from *a* to a_3 to the spectrum of *A*, and the simulated spectrum for $a_3 \rightarrow a$ was made by adding the simulated difference spectrum for electron transfer from a_3 to *a* to the inverse of the spectrum of *A*. The simulated spectra in *D* and *F* were constructed similarly to the corresponding panels (*C* and *E*), except that instead of using Gaussians, the deduced spectra for cytochromes *a* and a_3.

Table 2 shows a summary of four series of experiments with the pulsed enzyme, which is operationally defined as the form of the enzyme in which the two hemes become totally reduced. In addition to this distinction between the two forms of the enzyme, other differences are evident. 1) Four distinct kinetic phases are seen, in which significant electron redistribution takes place. 2) The second phase, in which an electron is transferred from cytochrome *a* to a_3, displays a rate constant about two orders of magnitude higher than seen for this transfer with the anaerobic resting enzyme. 3) There is a phase (number 3) which indicates a possible electron transfer from cytochrome a_3 to cytochrome *a*. In series 2b, an attempt was made to preform the pulsed enzyme prior to its mixing with reduced cytochrome *c* in the stopped-flow apparatus. To the anaerobic holding vessel containing the 20-nmol oxidized enzyme, 400 nmol of ascorbate, and 40 nmol of cytochrome *c*, 0.8 ml of air-saturated buffer (200 nmol O_2) was added in four steps (0.2 ml each). A final 0.6 ml of buffer (150 nM O_2) was then added, and the solution was flushed with N_2 until the O_2 electrode returned to a zero reading. The table shows that this treatment did speed the rates of the first two phases.

TABLE 1 Kinetic phases of the resting enzyme

			Reduced hemes	
	k	τ	a	a_3
	s^{-1}	s		
1	219 ± 100	0.0046	0.50	0
2	7.5 ± 3.2	0.13	0.56	0.06
3	1.1 ± 0.06	0.90	0.60	0.06
4	0.32 ± 0.04	3.1	0.66	0.16
5	0.05 ± 0.01	20	0.44	0.58

The data were averaged from three experiments in which the total level of reduction of cytochrome aa_3 was 50% (i.e., a total of one reduced heme) and in which the Gaussian analysis showed the time courses for electron distributions as illustrated in Fig. 1. The values for the kinetic and time constants were obtained by simultaneously fitting the time course vectors obtained in the SVD deconvolutions. The first phase kinetic constant is a pseudo-first order constant for a cytochrome *c* concentration which changed from 12.5 to 10 μM. Using a value of 11.2 μM, produces a second order rate constant of 2×10^7 M^{-1} s^{-1}. The amounts of reduced heme *a* and a_3 were obtained from the Gaussian analysis by equating 50% "pct*a*" and 50% "pcta_3" each to one heme *a* and one heme a_3.

DISCUSSION

In the first part of the discussion we will point out where the findings in the current work overlap those of earlier studies. Then some of the newer implications revealed in the present work are considered. In general, we hope to demonstrate that the techniques described here will be useful in the further study of this and similar kinetic processes in which many different spectra overlap.

Agreement of current findings with past studies

There is universal agreement that the first step in the reduction of cytochrome aa_3 by cytochrome *c* is the rapid bimolecular transfer of an electron from cytochrome *c* to cytochrome *a* and/or Cu_A. The bimolecular rate constant is reported to be $\sim 5 \times 10^6$ M^{-1} s^{-1} in 0.1 M phosphate at pH 7.4 and up to $\sim 10^8$ M^{-1} s^{-1} at low ionic strength (Brunori et al., 1988). In a summarization of past work, Wikström et al. (1981) make the following points. Only a single electron appears to be transferred by cytochrome *c* in the initial burst, regardless of the c/aa_3 ratio, and the single electron appears to be shared equally between heme *a* and Cu_A. The second phase in the resting enzyme is much slower ($k = \sim 0.5$ s^{-1})

TABLE 2 Kinetic phases of the pulsed enzyme

	k				τ			
	1	2	3	4	1	2	3	4
	s^{-1}				s			
1	217 ± 12 (7)	6.8 ± 1 (6)	0.12 ± 0 (2)	0.036 ± 0 (2)	0.0046	0.147	8.3	28
2a	120 ± 1 (4)	6.8 ± 0.7 (5)	0.13 ± 0 (5)	0.036 ± 0 (5)	0.0083	0.147	7.7	28
2b	309 ± 70 (2)	11.2 ± 0.1 (2)	0.13 ± 0 (2)	0.04 ± 0 (2)	0.0033	0.089	7.7	25
3	95 ± 7 (6)	3.4 ± 0.5 (6)	0.15 ± 0 (6)	0.04 ± 0 (6)	0.011	0.294	6.7	25

	Total reduced hemes			
	PD-Gaussians		PD-Spectra	
Kinetic phase	a	a_3	a	a_3
1	0.5–0.08	0	0.5	0.20
2	0.44	0.46	0.25	0.25
3	0.80	0.36	0.75	0.50
4	1.0	1.0	1.0	1.0

The kinetic data in the upper part of the table are averages of the number of experiments shown in parentheses. Four series of experiments are shown (rows) for which four kinetic phases were seen (columns). The first series included timecourses from 190-ms to 135-s duration. Only the first and second constants were resolved in incubations shorter than 1.4 s. Series 1, 2a, and 3 were conducted without pretreatment of the enzyme. For series 2b the enzyme was pretreted with reduced cytochrome *c* and O_2 as described in the text. The lower part of the table shows average amounts of each heme reduced at the end of each of the four kinetic phases determined by both the pseudoviruses deconvolution using Gaussians (PD-Gaussians) and using spectra (PD-Spectra). The first phase is essentially the transfer of an electron from cytochrome *c* to cytochrome *a*, and the fourth phase is the completion of the reduction of both hemes by electrons donated from cytochrome *c*. As discussed in the text, the extents of the changes in the two middle phases are determined by the amount of O_2 present. For the extends of hemes *a* and a_3 reduction shown in the table, the experiment shown in Fig. 3, *C* and 4*C*, was used.

(Brunori et al., 1988), and it involves the transfer of an electron from the heme a/Cu_A centers to the cytochrome a_3-Cu_B bimolecular center. Most stopped-flow studies concentrate on the events of the first few hundred milliseconds. Gibson and Greenwood (1965) produced data at "infinity," which was defined as 10 s. Table 3 presents a summary of past work on the kinetics of reduction of cytochrome aa_3 by cytochrome *c*. Using our criterion that the resting enzyme can be reduced to only a maximum extent of 50%, even after many seconds, the experiments of Gibson and Greenwood (1965) and of Andreasson et al. (1972) are listed as "resting enzyme." The second category, "pulsed enzyme," was used for cases where either a greater extent of reduction was seen, or where no claim for rigorous anaerobiosis was made and/or

TABLE 3 Previous studies on cytochrome aa_3 reduction by cytochrome *c*

Observed time	k_1 $c \rightarrow a$	k_2 $a \rightarrow a_3$	Wavelengths monitored	% reduced	Reference
	$M^{-1}\ s^{-1}$	s^{-2}	nm		
Resting enzyme *					
6.25 ms	3×10^6	0.5	445, 605	24 (aa_3)‡	Gibson and Greenwood (1965)
10 s				49 (aa_3)	
5 s	8×10^6		445, 550	33 (a)	Andreasson et al. (1972)
140 ms	8×10^6		550, 605	44 (a)	Andreasson (1975)
Pulsed enzyme					
200 ms	10^6–10^7		550, 605, 830	39 (aa_3)	Wilson et al. (1975)
105 ms	2×10^8		444	34 (aa_3)	Veerman et al. (1980)
300 ms	3×10^7	3§	445, 550, 603	80 (a) 0 (a_3)	Antalis and Palmer (1982)
2 s	10^8		563‖		Malatesta et al. (1990)

* The designation "Resting Enzyme" rests on the demonstration that less than 50% reduction of the enzyme occurs after several seconds of incubation. For incubations < 1 s, this is not established. The work of Andreasson (1975) is included because it was demonstrated in Andreasson et al. (1972), that the criterion was met.

‡ The percent reduction is expressed for either both hemes (aa_3) or for either heme (a) or heme a_3 alone (a_3). In all cases, the calculation was based on a reduced minus oxidized $\epsilon = 22\ mM^{-1}\ cm^{-1}$ at 605 nm and $\epsilon = 148\ mM^{-1}\ cm^{-1}$ at 445 nm for both hemes in cytochrome aa_3. For cytochrome *a*, either 80% of the 605-nm value or 50% of the 445-nm value was used. For cytochrome a_3, 20% of the value at 605 nm was used.

§ The value of 3 is higher than the value of ~0.05 reported here and of 0.5 reported by Gibson and Greenwood (1965), suggesting that perhaps some O_2 may have been present.

‖ In these experiments, the rate of oxidation of cytochrome *c* was followed. No data on cytochrome aa_3 were provided.

the period of observation too brief to allow a distinction. Our second order rate constant of $\sim 2 \times 10^7$ M^{-1} s^{-1} for the first electron transfer is in the range of earlier values. In all of these key papers, only two present a measured rate constant for the $a \rightarrow a_3$ electron transfer. One value, 0.5 s^{-1}, is from Gibson and Greenwood (1965), and the other, 3 s^{-1}, is from Antalis and Palmer (1982). These values are intermediate between the values of 0.05 s^{-1} that we found for the anaerobic resting enzyme and 11.2 s^{-1} for the most active pulsed form. Our finding that during the first 1000 ms of the time course for reducing cytochrome aa_3 by cytochrome *c*, little more than one electron out of four (or five) is transferred is also consistent with earlier findings. It is important to re-emphasize that the earlier research provides little or no experimental data on the sequential binding of the four electrons to the active redox centers of cytochrome aa_3.

New findings in the current studies

We find that the enzyme, in its resting state, binds only two electrons and that these appear to be held equally by all four centers, resulting in 50% reduction of each heme. The first electron is bound to the same extent and with essentially the same kinetics by both the anaerobic resting and the pulsed (O_2 exposed) enzyme (Tables 2 and 3). Up to the first second of incubation it is virtually impossible to distinguish between the former and latter states of the enzyme, without a global and dynamic method to differentiate cytochrome *a* from a_3. We have identified two experimental criteria which can distinguish between the anaerobic resting and pulsed forms of the enzyme. One is, as stated above, that with the resting enzyme, a maximum of only 50% reduction can be obtained. However, with the pulsed enzyme, the greater state of reduction is not seen in the first second. The second criterion is that the time constant for the $a \rightarrow a_3$ electron is ~20 s for the resting enzyme, and anywhere down to about 90 ms for different forms of the pulsed state. This very slow process would not be seen in the first second. It is extremely difficult to remove all traces of O_2 from the system. We have found that under the best of circumstances, a level of [O_2] of up to ~0.3 μM may be present. The K_m for O_2 binding to cytochrome aa_3 has been reported to be as low as 0.05 μM by Wikström et al. (1981) and in the range of 0.5 to 1.0 by Nicholls and Chance (1974). In our studies with cytochrome aa_3 liposomes, we have found that, under an Argon atmosphere, with a Davies-type O_2 electrode indicating complete anaerobiosis, there was still sufficient O_2 present to maintain the membrane potential at ~76% of its maximum value achieved at atmospheric O_2 levels in the presence of nigericin (Hendler et al., 1991). Therefore, even very low levels of [O_2] are sufficient to allow turnover of cytochrome aa_3. In the current work, we have taken steps to minimize the extent of O_2 contamination (e.g., the anaerobic pretreatment bottles and metal lines), we have carefully measured O_2 levels at every stage, and have identified effects due to O_2 presence (e.g., extents of reduction at late times and changes in kinetics). In most of the past studies reviewed above, it is not possible to know what amount of O_2 may have been present, especially since the results of O_2 presence are not sufficiently evident in the first second of incubation.

We have observed an "apparent" backflow of electrons from cytochrome a_3 to cytochrome *a*, with a time constant of 7–8 s, under our conditions. Although there is a valid reason for expecting such an event to occur (see Hendler and Westerhoff, 1992), there is an alternative explanation for the observed phenomenon. The appearance of the backflow phenomenon is made more pronounced by the presence of O_2. In fact, the more the O_2, the greater the apparent a_3 to *a* electron transfer. Also, the magnitude of the phenomenon is correlated to the magnitude of a concomitant cytochrome *c* oxidation (Figs. 3 and 4). The scheme in Fig. 8 can provide an explanation for these observations. The top of the figure shows events with the resting enzyme, in the absence of O_2. Only two electrons can be bound to the enzyme, and the *a* to a_3 transfer takes place with a kinetic constant of ~0.05 s^{-1}. In the presence of O_2, the half-reduced enzyme is brought into the cycle shown below the dotted line. In this cycle, the combination of steps 7 and 8 gives the appearance of an a_3 to *a* electron transfer, when in reality, the electrons leaving a_3 go to O_2 and the electrons going on to *a* come from *c*. The same phenomenon will result from a combination of steps 10 and 11. The operation of this cycle results in the consumption of cytochrome *c*. When the O_2 is consumed, the fully oxidized enzyme can proceed along two possible routes. If a sufficient number of turnovers has occurred, the enzyme transforms to the pulsed form and proceeds to 100% reduction. If not, the enzyme goes only to 50% reduction. At intermediate levels of O_2, a mixture of the two forms may exist. The scheme accounts for most of the observations, but it does

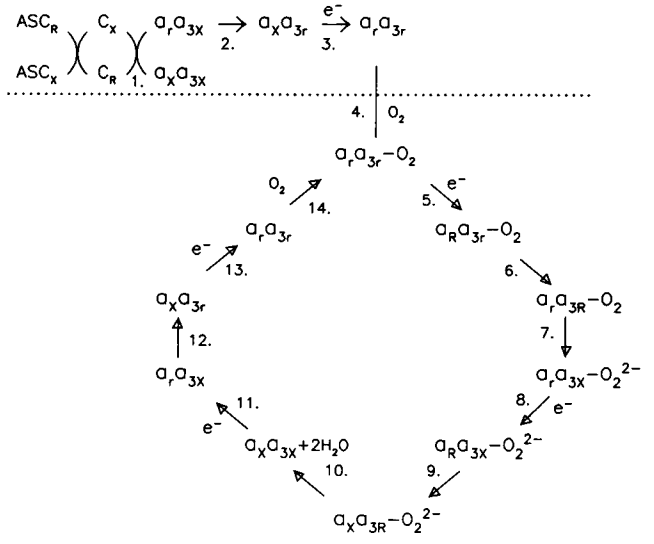

FIGURE 8 A model that can explain the observations made in these studies: The abbreviations ASC, C, and aa_3, represent ascorbate, cytochrome *c*, and cytochrome aa_3, respectively. The subscripts X, r, and R, represent the electron content of the individual center as 0, 1, and 2, respectively. The relation of this model to the experimental observations is discussed in the text.

not necessarily tell the whole story. In view of the evidence for redox cooperative interactions which result in an oscillation of the electron-binding affinities between cytochromes *a* and a_3 (Kojima and Palmer, 1983; Nicholls and Wrigglesworth, 1988; Di Cera, 1990; Nicholls, 1990; Hendler and Westerhoff, 1992), a temporary reversal of electron flow between cytochromes *a* and a_3 may still occur, and play an important role in the proton pumping process. A problem whose solution is not apparent in this scheme, is why the cytochrome *a* to a_3 electron transfer process is seen with a time constant near 0.1 s with the pulsed enzyme, if O_2 can only be bound in step 4 after the formation of the half reduced enzyme at ~20 s. What is needed is for O_2 to be bound by the enzyme holding only a single electron, so that the transformation by O_2 could happen much sooner. Evidence that the less reduced enzyme can bind O_2 has been presented (Shaw et al., 1978; Brzezinski and Malmström, 1985; Hendler, 1991).

Other considerations

It is known that the measured kinetic constants, after the binding of the first electron, are too low to account for the turnover of the enzyme. There are many factors which influence these rates. Two are the presence of appreciable levels of O_2, and the pulsed versus the resting state of the enzyme. For example, we have found that the rate constant for the cytochrome *a* to a_3 electron transfer was 0.05 s^{-1} for the anaerobic resting enzyme and 3–11 s^{-1} for various forms of the pulsed enzyme. With the pulsed enzyme, 10 turnovers just prior to the kinetic experiment, increased the first and second rate constants by factors of two to three. Another problem is the inability to maintain a constant rate of electron flow from cytochrome *c* throughout the whole time course. Ideally a very large c/aa_3 ratio should be used, but this makes it difficult to resolve the smaller aa_3 absorbances from the background of *c* absorbance. The presence of TMPD could help maintain an electron supply to *c* from ascorbate, but its optical contributions further complicate the resolution problem. We have chosen to use a supply of ascorbate without TMPD, but the slow time constant for the transfer of electrons from ascorbate to *c* (~6 s^{-1}) allows *c* to become limiting during the incubation. In spite of these problems, or challenges, the kinetic approach is valuable for helping to define the sequence of events during electron loading of the enzyme. This knowledge is essential in helping to set up a model that can account for the coupled electron and proton flows as the enzyme turns over in a membrane.

Future studies

To pursue the questions raised in the current work it is required that an instrument with increased capabilities be used. This instrument must be able to ensure complete O_2 exclusion whenever required. A double-mixing capability with rigorous control over the incubation period between the first and second mixings is needed to allow the prior formation of cytochrome aa_3 with limited and known electron content, and the subsequent exposure to precise amounts of O_2 at specific times. An instrument with these capabilities will be used to study conditions for formation of partially and fully pulsed states of the enzyme.

SUMMARY

1) The acquisition of multichannel kinetic data and their analysis by several types of global procedures are demonstrated.

2) The anaerobic resting enzyme can be reduced only to the extent of 50% regardless of the length of time of exposure to reduced cytochrome *c*. The two electrons are held equally among the two hemes and their associated Cu groups.

3) When a small amount of O_2 is present, 100% reduction of the enzyme is obtained. The time scale for full reduction, however, is in tens of seconds.

4) The binding of the first electron exhibits a time constant of <10 ms, and is indistinguishable in the cases of resting and pulsed enzymes.

5) The transfer of electrons from cytochrome *a* to cytochrome a_3 is clearly evident in all cases. The presence of O_2 speeds this transfer.

6) A simultaneous oxidation of cytochrome a_3 and reduction of cytochrome *a* is evident in cases where O_2 is present. This is most readily explained by the transfer of electrons from cytochrome a_3 to O_2, and from cytochrome *c* to cytochrome *a*.

REFERENCES

Andreasson, L. E. 1975. Characterization of the reaction between ferrocytochrome *c* and cytochrome *c* oxidase. *Eur. J. Biochem.* 53:591–597.

Andreasson, L. E., B. G. Malmström, C. Stromberg, and T. Vanngard. 1972. The reaction of ferrocytochrome *c* with cytochrome oxidase: a new look. *FEBS (Fed. Eur. Biochem. Soc) Lett.* 28:297–301.

Antalis, T. M., and G. Palmer. 1982. Kinetic characterization of the interaction between cytochrome oxidase and cytochrome c. *J. Biol. Chem.* 257:6194–6206.

Brunori, M., G. Antonini, F. Malatesta, P. Sarti, and M. T. Wilson. 1988. Structure and function of cytochrome oxidase: a second look. *Adv. Inorg. Biochem.* 7:93–153.

Brzezinski, P., and B. G. Malmström. 1985. The reduction of cytochrome *c* oxidase by carbon monoxide. *FEBS (Fed. Eur. Biochem. Soc) Lett.* 187:111–114.

Di Cera, E., 1990. Thermodynamics of local linkage effects: contracted partition functions and the analysis of site-specific energetics. *Biophys. Chem.* 37:147–164.

Gibson, Q. H., and C. Greenwood. 1965. The reaction of cytochrome oxidase with cytochrome c. *J. Biol. Chem.* 240:888–894.

Hendler, R. W. 1991. Can ferricyanide oxidize carbon monoxide-liganded cytochrome a_3? *J. Bioenerg. Biomembr.* 23:805–817.

Hendler, R. W., and Shrager, R. I. 1993. Deconvolutions based on singular value decomposition and the pseudoinverse: a guide for beginners. *J. Biochem. Biophys. Methods.* In press.

Hendler, R. W., and H. V. Westerhoff. 1992. Redox interactions in cytochrome *c* oxidase: from the "neoclassical" towards "modern" models. *Biophys. J.* 63:1586–1604.

Hendler, R. W., K. V. Subba Reddy, R. I. Shrager, and W. S. Caughey. 1986. Analysis of the spectra and redox properties of pure cytochromes aa_3. *Biophys. J.* 49:717–729.

Hendler, R. W., K. Pardhasaradhi, B. Reynafarje, and B. Ludwig. 1991.

Comparison of energy-transducing capabilities of the two- and three-subunit cytochrome aa_3 from *Paracoccus denitrificans* and the 13-subunit beef heart enzyme. *Biophys. J.* 60:415–423.

Kojima, N., and G. Palmer. 1983. Further characterization of the potentiometric behavior of cytochrome oxidase. *J. Biol. Chem.* 258:14908–14913.

Malatesta, F., P. Sarti, G. Antonini, B. Vallone, and B. Brunori. 1990. Electron transfer to the binuclear center in cytochrome oxidase: catalytic significance and evidence for an additional intermediate. *Proc. Natl. Acad. Sci. USA*. 87:7410–7413.

Nicholls, P. 1990. Control of proteoliposomal cytochrome *c* oxidase: the partial reactions. *Biochem. Cell Biol.* 68:1135–1141.

Nicholls, P., and B. Chance. 1974. Cytochrome *c* oxidase. *In* Molecular Mechanisms of Oxygen Activation. O. Hayaishi, editor. Academic Press, New York. 479–534.

Nicholls, P., and J. M. Wrigglesworth. 1988. Routes of cytochrome a_3 reduction: the neoclassical model revisited. *Ann. NY Acad. Sci.* 550:59–67.

Pardhasaradhi, K., B. Ludwig, and R. W. Hendler. 1991. Potentiometric and spectral studies with the two-subunit cytochrome aa_3 from *Paracoccus denitrificans*. Comparison with the 13-subunit beef heart enzyme. *Biophys. J.* 60:408–414.

Shaw, R. W., R. E. Hanson, and H. Beinert. 1978. Responses of the a_3 component of cytochrome *c* oxidase to substrate and ligand addition. *Biochim. Biophys. Acta.* 504:187–199.

Shrager, R. I., and R. W. Hendler. 1982. Titration of individual components in a mixture with resolution of difference spectra, pKs, and redox transitions. *Anal. Chem.* 54:1147–1152.

Veerman, E. C. I., J. Wilms, G. Casteleijn, and B. F. Van Gelder. 1980. The pre-steady state reaction of ferrocytochrome *c* with the cytochrome *c*-cytochrome aa_3-complex. *Biochim. Biophys. Acta.* 590:117–127.

Wikström, M., K. Krab, and M. Saraste. 1981. Cytochrome oxidase. A synthesis. Academic Press, New York.

Wilms, J., J. L. M. L. Van Rijn, and B. F. Van Gelder. 1980. The effect of pH and ionic strength on the steady-state activity of isolated cytochrome *c* oxidase. *Biochim. Biophys. Acta.* 593:17–23.

Wilson, M. T., C. Greenwood, M. Brunori, and E. Antonini. 1975. Kinetic studies on the reaction between cytochrome *c* oxidase and ferrocytochrome *c*. *Biochem. J.* 147:145–153.

Yoshikawa, S., M. G. Choc, M. C. O'Toole, and W. S. Caughey. 1977. An infrared study of CO binding to heart cytochrome *c* and hemoglobin A. *J. Biol. Chem.* 252:5498–5508.